



Bullet Points

- Imaging recommendations appropriate for anatomical regions
- Selection of pathologies with cranial nerve involvement
- Cases

Introduction

Magnetic resonance imaging (MRI) is the main imaging modality in the diagnostic workup of neurologic symptoms regarding cranial nerves. Superior soft tissue contrast and advanced MRI techniques allow a thorough assessment of the nervous system. With appropriate sequences, 3 T MRI systems offer a better signal-to-noise ratio and superior spatial resolution. Due to many medical and nonmedical reasons, MRI systems with 1.5 T are more common. In short, systems with 3 T are more cost-intensive as they are technically more demanding. For most anatomical regions, any MRI system requires a dedicated radiofrequency coil, which has to be changed if an examination exceeds the anatomical range of the specific coil. MRI is a safe examination tech-

nique. However, checking patient history for metal foreign objects or incompatible implants is time-consuming. Websites offer a thorough database free of charge, e.g., www.MRIsafety.com/list.html. For several examinations, intravenous contrast agents are not necessary. In some cases, the examination protocol must be adapted after evaluation of the first sequences, and application of a contrast agent may be necessary. Sedation with an appropriate monitoring can be helpful for patients with claustrophobia and infants but demands much organizational effort.

Direct visualization of nerves is possible. Due to the small size and complex surroundings, the depiction of most cranial nerves in the extracranial segments is difficult and strongly depends on the anatomical region. In all cases, MRI visualizes the presumed pathway of the nerve. With high sensitivity, MRI depicts denervation edema in muscles. The pattern of denervated muscles in turn may indicate the affected nerve. A reliable depiction of perineural spread of neoplastic processes is a unique and valuable feature of MRI and is essential in the staging of head and neck cancer.

The role of computed tomography (CT) in the diagnostic workup of cranial nerve pathologies is very limited. Processes in cranial nerve nuclei or tracts, e.g., infarction or hemorrhages, are depicted identically to processes in other parts of the central nervous system, with commonly known weaknesses in comparison to

Authors of this chapter: Stefan Meng and Barbara Horvath-Mechtler.

MRI. Although the spatial resolution of standard CT systems is superior to standard MRI systems, the much lower soft tissue contrast limits CT to the visualization of osteolytic, osteoblastic, or traumatic processes of the skull base. A direct visualization of a cranial nerve either intra- or extracranially is not feasible.

Ultrasound is a cost-effective, high-resolution imaging modality. There are virtually no contraindications for diagnostic ultrasound. Natural limitations are the bone barrier, gas-filled spaces, and nerves lying deeply in the body. Thus, intracranial and intraosseous segments of cranial nerves cannot be examined in clinical routine. Just outside the skull base, some of the cranial nerves may be directly visualized by ultrasound. Deep lying nerves can be reached by ultrasound using low frequencies only, which in turn yield low resolution images [1]. While the course of the vagus nerve in the neck can be visualized easily by ultrasound, the branches in the abdomen cannot be routinely examined. In addition to bones, gas also represents an absolute barrier for ultrasound, so the course of the vagal branches in the thorax is invisible for ultrasound. Unfortunately, ultrasound of nerves has not been established as a standard tool in many clinical facilities. This might be due to the limitation that ultrasound is strongly dependent on the skills of the examiner.

In this chapter, we will provide a concise radiological overview of imaging for each cranial nerve. Imaging modalities will be discussed regarding the respective anatomical segment. For selected diseases, we also present imaging modality recommendations. Finally, special regions will be discussed.

Cranial Nerve I: Olfactory Nerve

Using MRI, depiction the olfactory mucosa of the nasal cavity is feasible, but the diagnostic value exceeding the possibilities of an endoscopy might depend on the individual case.

The osseous structure of the nasal cavity and the paranasal sinuses as well as the base of the

anterior fossa – especially of the cribriform plate – are adequately examined by CT [2].

Although visualization of the fila olfactoria is technically feasible in experimental settings using high-resolution MRI systems, the detection of a traumatic rupture of these thin structures is not a routine examination [3].

The olfactory system, beginning at the bulb of the olfactory nerve, can be routinely visualized by MRI systems with a field strength of 1.5 and 3 T. Here, T2-weighted images show a strong contrast between the bright cerebrospinal fluid and the dark nervous structures. At the same time, there is poor contrast between the individual nervous structures of the olfactory system, the brain, and local bone structures [2].

Congenital anosmia: MRI is the imaging modality of choice for delineation of hypoplastic or even absent olfactory bulbs (Fig. 2.1).

Local tumor process: MRI and CT, both with contrast, are necessary to assess the intra- and extracranial tumor extent. MRI is necessary to evaluate the soft tissue and CT is necessary for detection of bone destruction (Fig. 2.2).



Fig. 2.1 Olfactory nerve aplasia. Coronal T2w MRI. Olfactory bulb aplasia on the patient's left side (arrow) and regular anatomical situation on the right side (arrowhead)



Fig. 2.2 Medulloblastoma. Coronal T2w MRI. Patient with an medulloblastoma which is extending into the olfactory nerve on the left side (arrows). Regular nerve on the right patient side (arrowhead)

Cranial Nerve II: Optic Nerve

Due to motion, ocular globes are difficult to scan with high resolution MRI. Technically, ophthalmic ultrasound can visualize the posterior segment of the eye, retina, and the macula as well as the beginning of the optic nerve. Optic nerve

head drusen, detachments of the retina, and tumors can be detected. Furthermore, ultrasound is able to detect elevated intracranial pressure, which leads to a widening of the optic nerve sheath [4].

The method of choice for the intraorbital segment of the optic nerve and its surroundings is MRI. The use of contrast agent is advised in most cases as the optic nerve shows no enhancement; thus, enhancing pathological processes may support easier detection. The orbital wall and the optic canal are assessed best with CT and multiplanar reconstructions.

MRI is the best modality for the intracranial part of the optic nerve, the optic chiasm, and the optic tracts. High-resolution 3D T1- and T2-weighted sequences are recommended. 3D reformations simplify the assessment of the visual pathway [5]. Diffusion tensor imaging may depict the composition of the nerve fibers.

Idiopathic orbital inflammation: The recommended imaging modality is MRI with contrast, which shows inflammatory changes in the orbital soft tissue. Alternatively, CT with contrast may be used.

Optic neuritis: The best imaging modality is MRI with contrast. Alternatively, sequences without contrast (T2w with fat saturation) might be helpful. Considering possible underlying diseases, such as neuromyelitis optica or multiple sclerosis, extension of the field of view to the entire brain is recommended (Fig. 2.3)

Graves disease: For surgical planning, CT as well as MRI are indicated.

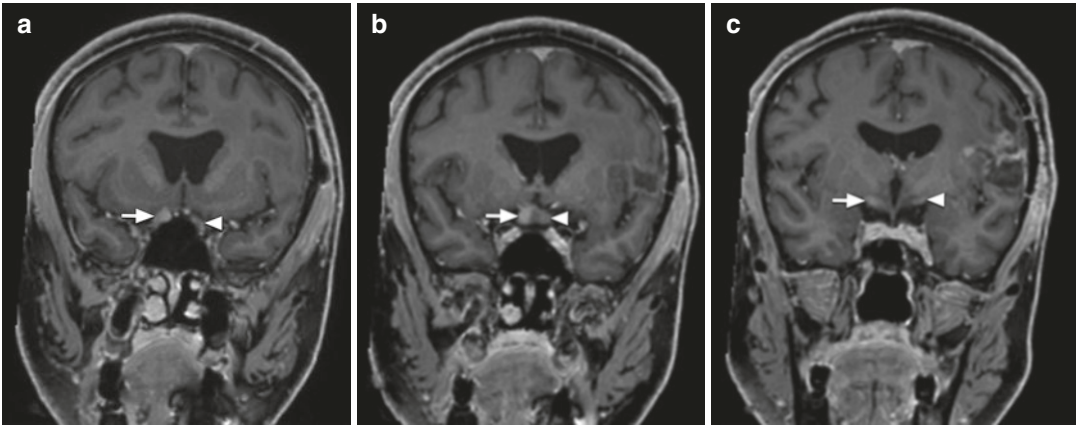


Fig. 2.3 Optic neuritis. Coronal T1w MRI with contrast. Marked enhancement of the right visual pathway (arrows) and regular depiction on the left side (arrowheads). (a) optic nerve; (b) optic chiasm; (c) optic tract

Cranial Nerve III: Oculomotor Nerve

The course of the oculomotor nerve can be divided into seven segments, which are the mesencephalon, interpeduncular cistern, petroclinoid segment, trigonal segment, cavernous segment, fissural segment, and orbit.

For the mesencephalic to the cavernous segment, MRI with high-resolution T2w sequences in axial and coronal planes are advised. In the cavernous segment, the nerve lies within the lateral wall of the cavernous sinus just below the anterior clinoid process (Fig. 2.4). Of all cranial nerves (oculomotor, trochlear, ophthalmic, and maxillary) in the lateral wall, the oculomotor nerve is the most superior [6].

The oculomotor nerve enters the orbit via the superior orbital fissure. Bony structures should be assessed by CT. Depiction of the oculomotor nerve divisions in the orbit may be difficult.

Aneurysms: Due to the close proximity of the oculomotor nerve to the posterior communicating artery, posterior cerebral artery, and the superior cerebellar artery, isolated symptoms of the oculomotor nerve indicate the search for an aneurysm of the arteries, preferably with MRI or alternatively with CT.

Uncal herniation: In cases of trauma to the head, an isolated lesion of the oculomotor nerve might result from a nerve entrapment by uncal herniation. MRI is the imaging modality to assess any brain parenchyma dislocation.

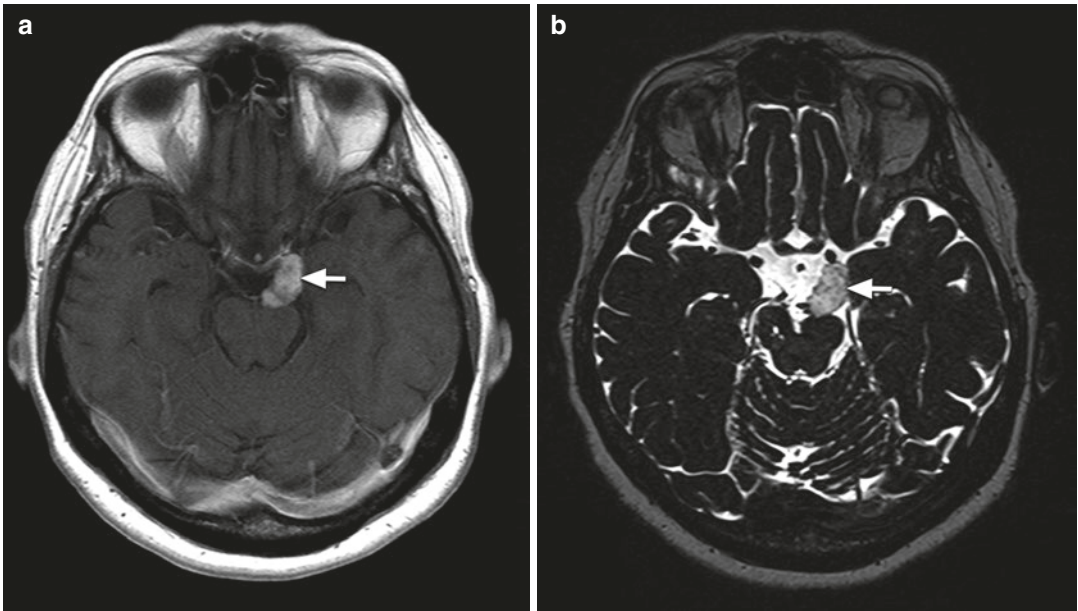


Fig. 2.4 Oculomotor nerve schwannoma. (a) Axial T1w contrast-enhanced MRI. (b) Axial space MRI. Bulky, enhancing oculomotor nerve schwannoma on the left side (arrow)

Cranial Nerve IV: Trochlear Nerve

The nuclei of each trochlear nerve lie contralateral to the side of the course and muscle of the nerve.

Inferior to the colliculus, the nerve leaves the brain stem as the only cranial nerve exiting from the brain stem dorsally. Through the quadrigeminal and ambient cistern, the nerve travels frontal between the posterior cerebral artery and the superior cerebellar artery (Fig. 2.5). From below the edge of the tentorium, the nerve enters the lateral wall of the cavernous sinus just below the course of the oculomotor nerve. Finally, the nerve enters the orbit via the superior orbital fissure above the annulus of Zinn. The course of the nerve from the nuclei to the superior orbital fissure can be visualized by MRI. Direct visualization of the nuclei is not possible. Due to the small size of the nerve, visualization of the nerve can be challenging. High-resolution sequences in coronal and axial planes are recommended. Bony structures are depicted best with CT.



Fig. 2.5 Regular trochlear nerve depiction. Axial space MRI. Routine depiction of the trochlear nerve may be demanding as demonstrated here. The course of the nerve (arrow) is just visible

Isolated lesions of the nerve are based on trauma. Complex neuropathies with the association of other local cranial nerves occur due to tumors, stroke, and processes in the cavernous sinus or orbit [7].

Aneurysm: Isolated lesions of the trochlear nerve might result from an aneurysm of the superior cerebellar nerve. Here, MRI is the primary imaging modality, and the secondary modality is CT.

Trauma: Injuries of the trochlear nerve due to trauma may be assessed with MRI.

Cranial Nerve V: Trigeminal Nerve

The origin of the trigeminal nerve is in the mesencephalon, pons, and the medulla oblongata as well as the cervical spinal cord (Fig. 2.6). In the cisternal segment, the nerve lies in the prepontine cistern. Then, the trigeminal nerve lies as a trigeminal ganglion in a dural space called Meckel's cave. In the abovementioned segments, the trigeminal nerve can be examined with MRI.

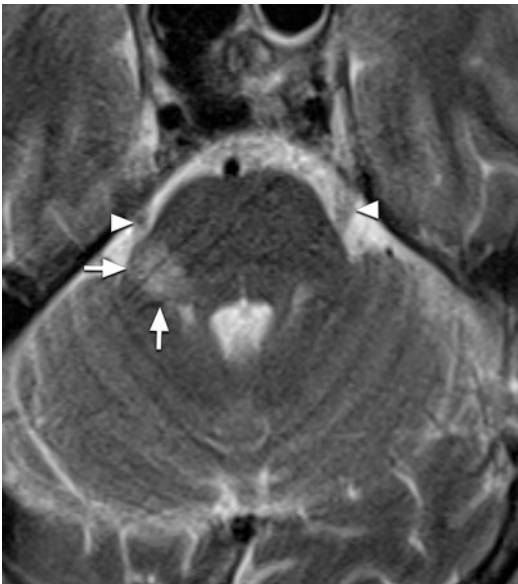


Fig. 2.6 Multiple sclerosis plaque in trigeminal nuclei. Axial T2w MRI. Multiple sclerosis plaque in the right intra-axial trigeminal nerve origin (arrows). Regular trigeminal nerve roots on both sides (arrowheads)

At the trigeminal ganglion, the three branches of the trigeminal nerve separate and head to different directions:

1. The ophthalmic branch (V1) enters the lateral wall of the cavernous sinus just below the trochlear nerve and enters the orbit via the superior orbital fissure. For the cavernous sinus, MRI is the primary modality. In the orbit, direct visualization of the ophthalmic nerve branches is difficult. The tiny sensory terminal branches of the ophthalmic nerve, the supraorbital and supratrochlear branches, can be examined directly with high resolution ultrasound beginning at the superior rim of the orbit into the periphery.
2. The maxillary branch (V2) also enters the lateral wall of the cavernous sinus below the ophthalmic branch. Again, MRI is the modality of choice. The maxillary branch enters the foramen rotundum, passes the superior part of the pterygopalatine fossa, and enters the orbital region through the inferior orbital fissure. In the orbital floor, the nerve travels frontally in the infraorbital canal (Fig. 2.7)



Fig. 2.7 Maxillary fracture. Axial CT. Fracture of the maxilla on the right side with air-fluid level in the right maxillary sinus (white asterisk). The infraorbital canal is also affected (arrow), while the canal is intact on the left side (arrowhead)

From the foramen rotundum to the infraorbital canal, CT depicts the bony walls of the pathway and MRI of the soft tissue. Leaving the infraorbital canal, the branches of the infraorbital nerve course into the soft tissue of the face, where the nerve branches can be assessed directly with high-resolution ultrasound.

3. The mandibular branch (V3) does not enter the cavernous sinus. Instead, the nerve passes through the foramen ovale into the masticatory space, where it supplies the motor branches for the pterygoid muscles and the muscle of the soft palate. For the passage through the skull base, CT is the best modality. Below the base of the skull direct visualization of the mandibular nerve branches is not possible. However, the anatomical surroundings of the known nerve branch pathways can be assessed with MRI. Peripheral branches, which may be directly visualized, are branches on the surface of the head, such as the auriculotemporal masseteric nerve. The bony canal and the inferior alveolar nerve itself can be visualized by CT and MRI, respectively. The superficial segment of the auriculotemporal nerve and of the masseteric nerve can be examined with high-resolution ultrasound [8].

Trigeminal neuralgia: Blood vessels with contact to the trigeminal nerve are visualized best with high-resolution MRI [9].

Inflammation: Local infections can be visualized with MRI and contrast enhancement.

Cranial Nerve VI: Abducens Nerve

Originating from the abducens nuclei in the pons, the nerve leaves the brain stem in a groove between the pons and the medulla oblongata. For assessing the pons, MRI is the imaging modality of choice.

In the prepontine cistern and cavernous sinus, the nerve lies in the center, lateral to the internal carotid artery. Here, the nerve is visualized best by MRI, where in most cases due to the anatomical course of the nerve, 3D reconstructions might be necessary (Fig. 2.8). Passing through the superior orbital fissure and orbit, the nerve may be depicted directly by MRI and CT, with the latter for the bony walls adjacent to the nerve.

Petrous apicitis/Gradenigo syndrome: The inflammatory changes, which extend from the middle ear into the pneumatized petrous apex, might also affect the trochlear nerve. CT depicts the bony destruction, whereas MRI proves the meningeal thickening [10] (Fig. 2.9).

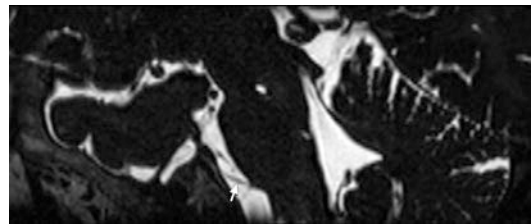


Fig. 2.8 Regular abducens nerve. Sagittal space MRI reconstruction. As the course of the nerve (arrow) is not aligned to the typical axial, sagittal, or coronal scanning plane, 3D reconstructions are often necessary to visualize the nerve longitudinally

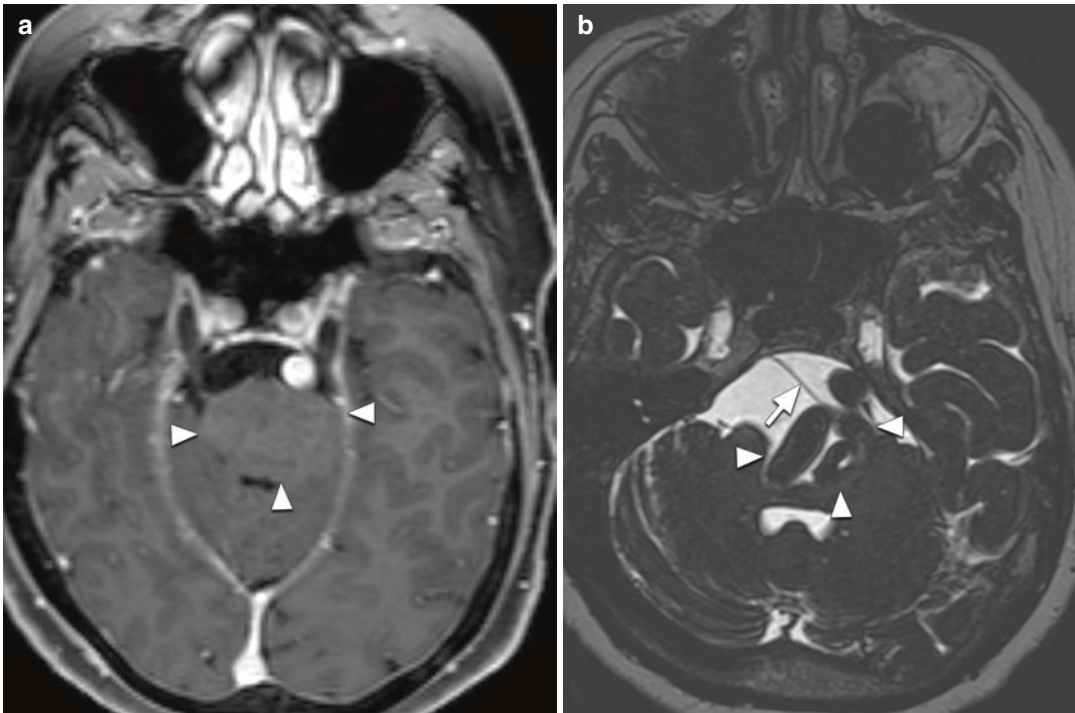


Fig. 2.9 Bulging of the abducens nerve by a vascular malformation. (a) Axial T1w MRI with contrast. (b) Axial space MRI. A voluminous vascular malformation (arrow-

heads) leads to a bulging of the right abducens nerve (arrow) to the left side

Cranial Nerve VII: Facial Nerve

The intra-axial origins of the facial nerve lie in the pons and medulla oblongata. The facial nerve leaves the brain stem at the cerebellopontine angle. In the cisternal segment, the larger motor root lies anterior and the smaller sensory posterior. Together with the vestibulocochlear nerve, the facial nerve enters the internal auditory canal. MRI is the best imaging modality for the segments from the brain stem to the internal auditory canal. In the latter, CT may be used to depict the bony boundaries. In the temporal bone, the course of the facial nerve can be divided into internal auditory canal, labyrinthine, tympanic, and mastoid segment. After application of contrast agent, the nerve may be depicted directly by MRI. Leaving the skull base at the stylomastoid foramen, the facial nerve gives off its motor

branches in the parotid gland. The chorda tympani joins the lingual nerve.

Starting at about 1 cm below the opening of the stylomastoid foramen, the motor branches of the facial nerve in the parotid gland can be directly visualized with high-frequency ultrasound and high-resolution MRI. Depicting the tiny branches into the periphery of the nerve well outside the parotid gland is feasible with high-resolution ultrasound (Fig. 2.10) [11].

Bell's Palsy: MRI may depict contrast enhancement of the facial nerve on the symptomatic side. Ultrasound may depict thickening of the facial nerve in the parotid gland (Fig. 2.11).

Schwannoma: Both MRI and ultrasound depict the well-circumscribed tumor. To assess the tumor extent at the stylomastoid foramen, MRI is the best imaging modality (Fig. 2.12).

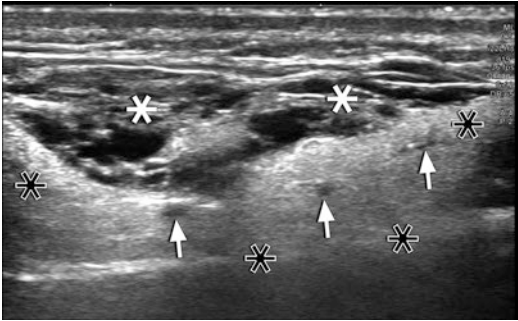


Fig. 2.10 Hyaluronic acid depositions in the parotid gland. Coronal ultrasound of the parotid gland. The patient originally underwent hyaluronic acid filler injections for cosmetic reasons. The original target region was the dermis. Inside the parotid gland (black asterisks), hypoechoic hyaluronic acid depositions (white asterisks) can be seen. Close to these depositions are the peripheral branches of the facial nerve (arrows)

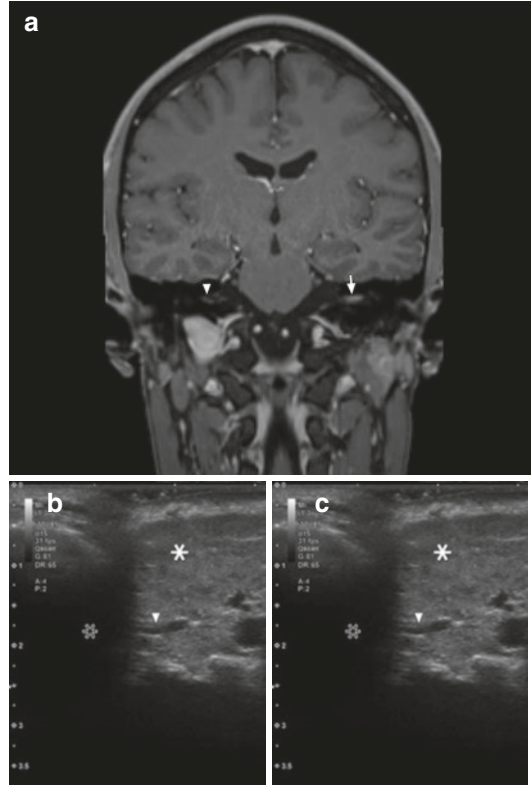


Fig. 2.11 Bell's palsy. (a) Coronal T1w MRI with contrast. On the symptomatic left side, contrast enhancement of the facial nerve (arrow) in the temporal bone is markedly stronger compared to the asymptomatic right side (arrowhead). (b) Para-axial ultrasound of the parotid gland. The facial nerve on the symptomatic side is swollen (arrow) compared to the asymptomatic side (arrowhead). (c) Mastoid process (Back asterisk), parotid gland (white asterisk)

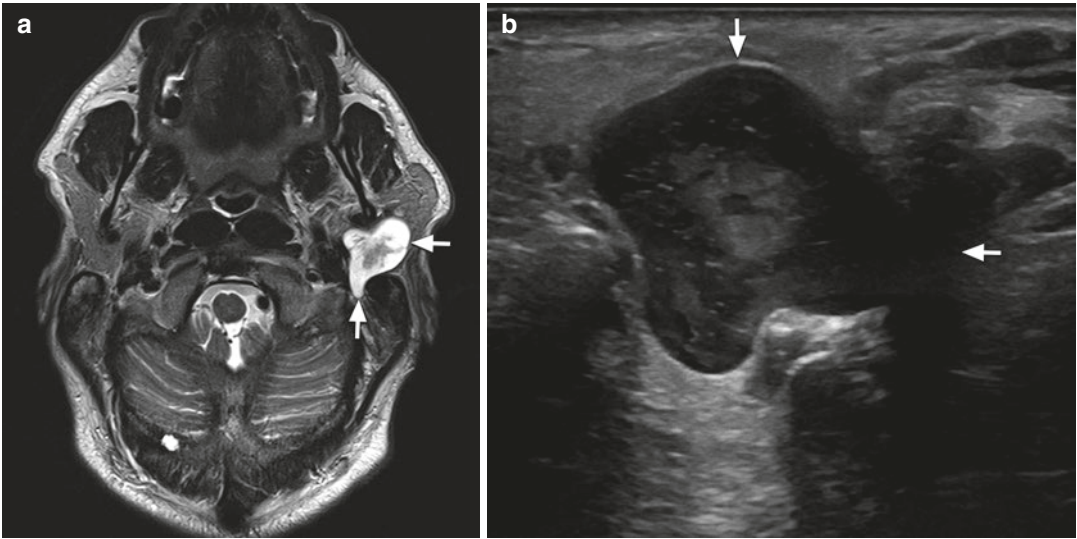


Fig. 2.12 Facial nerve schwannoma. (a) Axial T2w MRI, (b) para-axial ultrasound of the parotid gland. Large schwannoma (arrows) in the parotid gland of the left side

Cranial Nerve VIII: Vestibulocochlear Nerve

The first cochlear nuclei lie in the inferior cerebellar peduncle. The cochlear part of the vestibulocochlear nerve enters the brain stem at the cerebellopontine angle. In the cerebellopontine angle, the cochlear nerve forms the vestibulocochlear nerve with the vestibular nerve. In the temporal bone, the cochlear part lies in the anterior inferior quadrant of the internal auditory canal, which the nerve enters from the cochlea, where it is situated in the central axis of the spiral.

The vestibular fibers enter the brain stem at the cerebellopontine angle. In the cerebellopontine cistern, the vestibular part of the vestibulocochlear nerve lies posterior to the cochlear nerve.

The brain stem and the cisternal section of the nerve are visualized with MRI. The entire temporal section of the nerve can be examined with CT and MRI, depending on the suspected pathology. Contrast agent application is recommended.

Schwannoma: High-resolution MRI depicts the nerve in the entire segment from the cerebellopontine angle into the internal auditory canal (Fig. 2.13) [12].

Ramsay Hunt syndrome: With MRI the contrast enhancement of the vestibulocochlear nerve can be detected.

Metastases: Local metastases may also be visualized best with MRI with contrast. Alternatively, CT with contrast may be used.

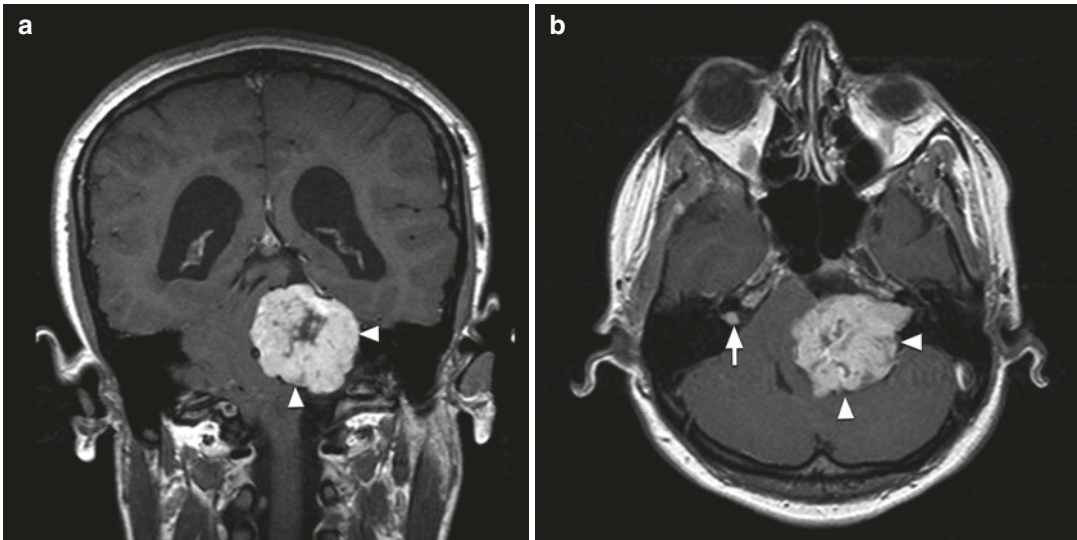


Fig. 2.13 Schwannoma and meningioma. (a) Coronal T1w MRI with contrast, (b) Axial T1w MRI with contrast. Large meningioma on the left side (arrowheads). Schwannoma of the vestibulocochlear nerve on the right side (arrow)

Cranial Nerve IX: Glossopharyngeal Nerve

The nuclei of the glossopharyngeal nerve lie in the medulla oblongata. In the retroolivary sulcus, the nerve leaves the brain stem and enters the basal cistern with the vagus nerve and the bulbular part of the accessory nerve (Fig. 2.14). In the anterior part of the jugular foramen, the nerve has its superior and inferior sensory ganglia. In the anterior part of the carotid space, the nerve passes lateral to the internal carotid artery to the neck and gives off branches to the lingual nerve, to the tympanic branch, to the stylopharyngeus branch, to the carotid sinus, and to the pharynx.

For visualization of the intracranial part, MRI and CT are necessary. The extracranial part of the glossopharyngeal nerve cannot be depicted directly. Unfortunately, the examination is limited to the visualization of the assumed regular course of the nerve [13] (Fig. 2.15).

Glossopharyngeal compression: Vascular compression by the posterior inferior cerebellar artery and anterior inferior cerebellar artery are examined best by high-resolution MRI.

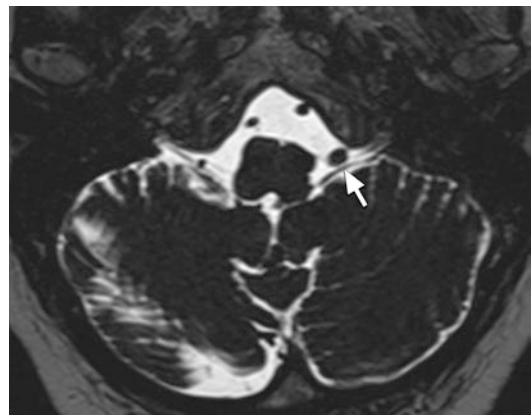


Fig. 2.14 Regular glossopharyngeal nerve. Axial space MRI. Regular course of the glossopharyngeal nerve on the left side (arrow)

Eagle syndrome: For this rare syndrome with compression of the glossopharyngeal nerve by an elongated styloid process, CT depicts the osseous situation (Fig. 2.16).

Schwannoma jugular foramen: For delineation of the soft tissue, MRI is the best imaging modality, and for the osseous borders, CT is the best imaging modality.

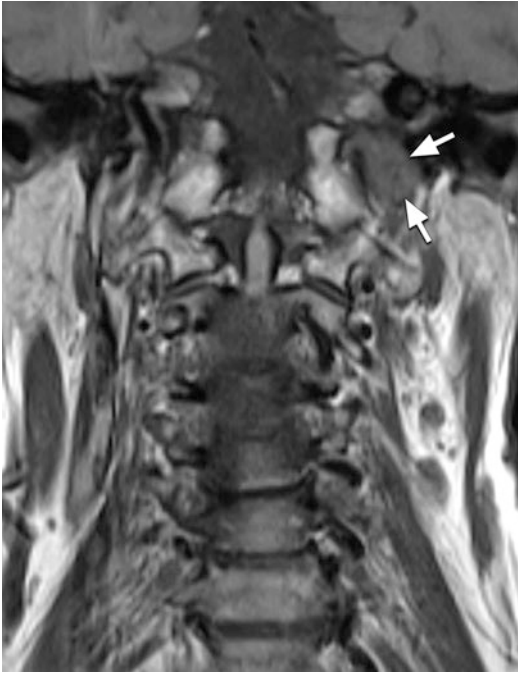


Fig. 2.15 Glomus tumor. Coronal T1w MRI. Ovoid-shaped, glomus jugulare tumor (arrows) right below the jugular foramen on the left side

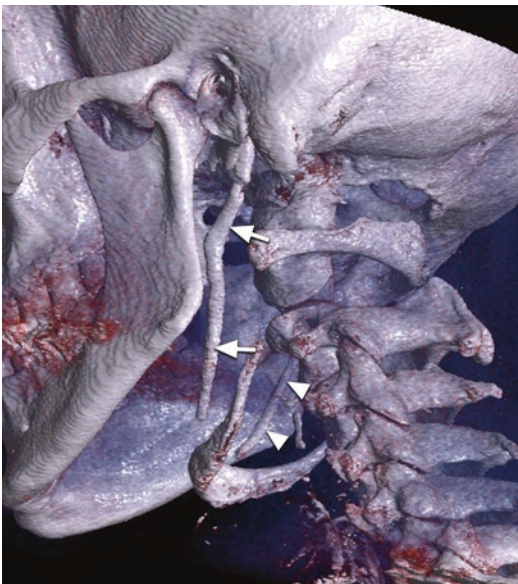


Fig. 2.16 Eagle syndrome. 3D reconstruction of a CT scan. The excessively long styloid processes on both sides (arrows) almost come in contact with the hyoid bone

Cranial Nerve X: Vagus Nerve

The nuclei of the vagus nerve lie in the medulla oblongata. Along with the glossopharyngeal nerve, the vagus nerve exits the brain stem at the retroolivary sulcus. Via the jugular foramen, the vagus nerve passes through the skull base. Below the skull base, the nerve lies in the carotid space. Along the posterior side of the carotid artery, the nerve enters the thorax, where the right nerve is located anterior to the right subclavian artery and the left nerve anterior to the aortic arch. Via a plexus around the bronchi, the nerve fibers enter the lungs, and around blood vessels, the nerve innervates the heart. The nerve also forms a plexus around the esophagus. Via this plexus, the nerve also reaches the abdomen and provides innervation for the intestines, from the stomach to the left colon flexure.

For the nerve segments in the brain, the subarachnoidal space, and skull base, MRI is the best imaging modality. In the neck, the main trunk of the vagus nerve can be partially visualized with ultrasound. The segments in the thorax and abdomen cannot be directly depicted. CT or MRI may visualize the regular pathway and surrounding of the nerve [14].

Glomus vagal paraganglioma: In the region 1–2 cm below the jugular foramen equally contrast-enhanced CT and MRI are recommended.

Schwannoma: If the location of the tumor is accessible, ultrasound is the best imaging modality. If the location is 1–2 cm below the jugular foramen MRI with contrast is recommended. With CT the scalloping of the jugular foramen may be detected (Fig. 2.17).

Neurofibroma: MRI with contrast is the best imaging modality. If accessible ultrasound can be used to directly visualize the neurogenic origin of the tumor. Sequences with strong T2-weighted signal and low signal from fat tissue may be used to search for neurofibromas.

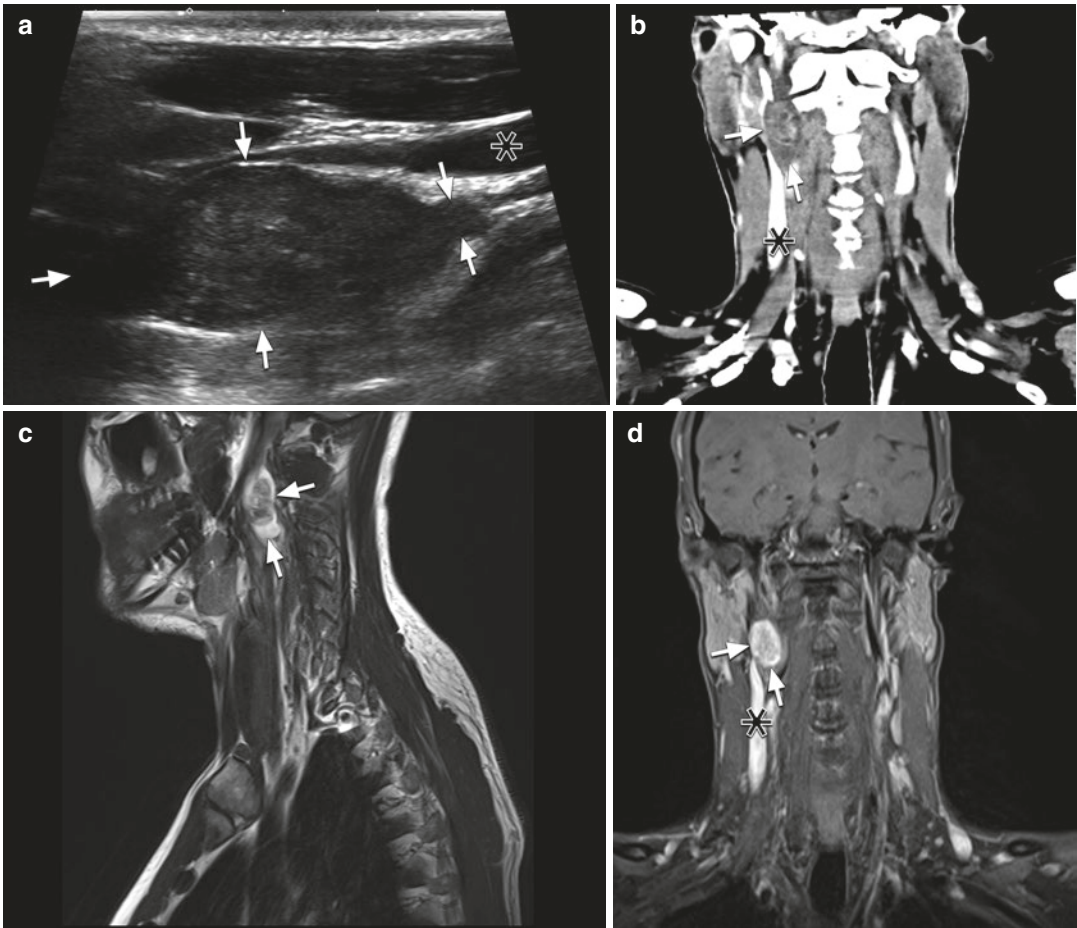


Fig. 2.17 Vagus nerve schwannoma. (a) Coronal ultrasound of the schwannoma at the neck, (b) coronal CT with contrast of the neck, (c) sagittal T2w MR, (d) coronal T1w with fat saturation MRI with contrast. Schwannoma

(arrows) of the vagus nerve in the cranial part of the neck. Partially compressed internal jugular vein (black asterisks)

Cranial Nerve XI: Accessory Nerve

For the intra-axial and subarachnoidal segments, MRI is the best imaging modality. The accessory nerve originates from the medulla oblongata and from the cervical spinal cord. The fibers from the medulla oblongata exit the brain stem at the retrolivary sulcus. The fibers from the cervical spine exit the cervical cord between the ventral and dorsal roots and course cranially in the spinal canal.

CT provides depiction of the skull base. In the foramen magnum, the fibers unite and merge

with the fibers from the medulla oblongata. Via the basal cistern and the jugular foramen, the accessory nerve leaves the skull. The fibers originating from the medulla oblongata merge with the vagus nerve, and the branches from the cervical spinal cord go to the sternocleidomastoid and trapezius muscle.

Extracranial segments of the nerve may be examined indirectly with MRI and directly with high-resolution ultrasound. With MRI, the supposed, regular nerve pathway and the specific target muscles of the nerve may be assessed, whereas high-resolution ultrasound visualizes

the nerve directly from 1–2 cm below the inferior surface of the skull base to branches of the nerve within the muscles [15].

Injury: Ultrasound is the best imaging modality to visualize the nerve in the neck region. From 1–2 cm below the jugular foramen to the trapezius muscle, the nerve and its surround can be assessed with superior spatial resolution. High-resolution MRI may also be used to examine the course of the nerve (Figs. 2.18 and 2.19).

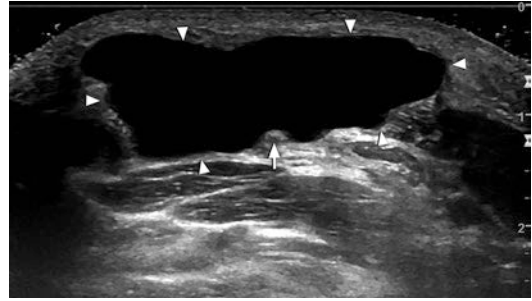


Fig. 2.18 Nerve compression by a seroma. Axial ultrasound of the accessory nerve at the lateral side of the neck. Compression of the accessory nerve (arrow) by a postoperative seroma (arrowheads) following a diagnostic excision of a lymph node

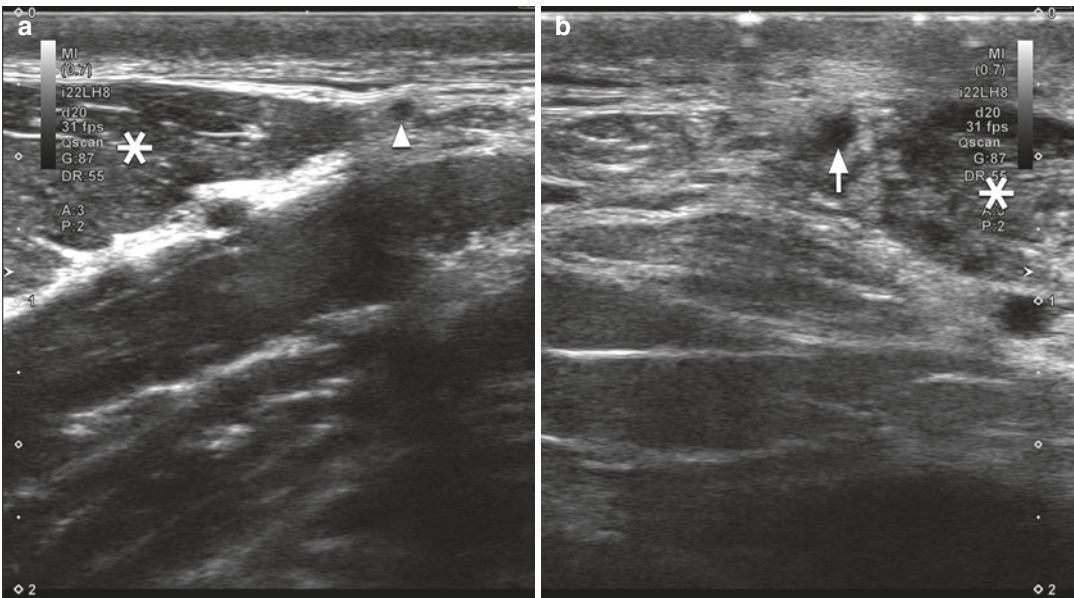


Fig. 2.19 Postoperative neuroma. Axial ultrasound of the accessory nerve (a) at the asymptomatic lateral side of the neck and (b) at the symptomatic lateral side of the neck.

After surgical removal of a lipoma, the accessory nerve is swollen over a segment of several centimeters resulting in a severe shoulder lift weakness

Cranial Nerve XII: Hypoglossal Nerve

For the medullary origin, MRI is the modality of choice. The hypoglossal nuclei lie in the medulla oblongata in a posterior, paramedian position.

In the subarachnoid segment, MRI is also standard. Leaving the brain stem anterolaterally, multiple rootlets of the hypoglossal nerve converge to one nerve in the subarachnoid space. Close to the hypoglossal canal, the hypoglossal nerve is adjacent to the course of the vertebral artery, which is located medial to the nerve.

The hypoglossal canals are directed laterally. The canals may have osseous spurs or may be divided unilaterally. For the assessment of the bony structure of the skull base, the use of CT is advised. MRI might pick up pathologic contrast enhancement of the nerve (Fig. 2.20).

Outside the skull, MRI provides visualization of the supposed pathway of the nerve. High-

resolution ultrasound picks up the nerve directly, although ultrasound cannot routinely reach the nerve close to the inferior side of skull base. In the submental and oral region, visualization of the hypoglossal nerve is excellent with high-resolution ultrasound. Beginning at the carotid sheath, the course of the nerve can be picked up by ultrasound and tracked into the body of the tongue. Inside the tongue, branching of the hypoglossal nerve can be partly visualized (Figs. 2.21 and 2.22).

Visualization of the tongue muscles facilitates adapting the diagnostic algorithm. Denervation edema and atrophy may direct the clinical focus to the hypoglossal nerve [16].

Malignant tumor progression: Entrapment or Infiltration by neoplastic processes in the neck can be examined best by MRI for the cervical region below the skull base. Especially in the lower region at the jaw and tongue, ultrasound has superior spatial resolution.

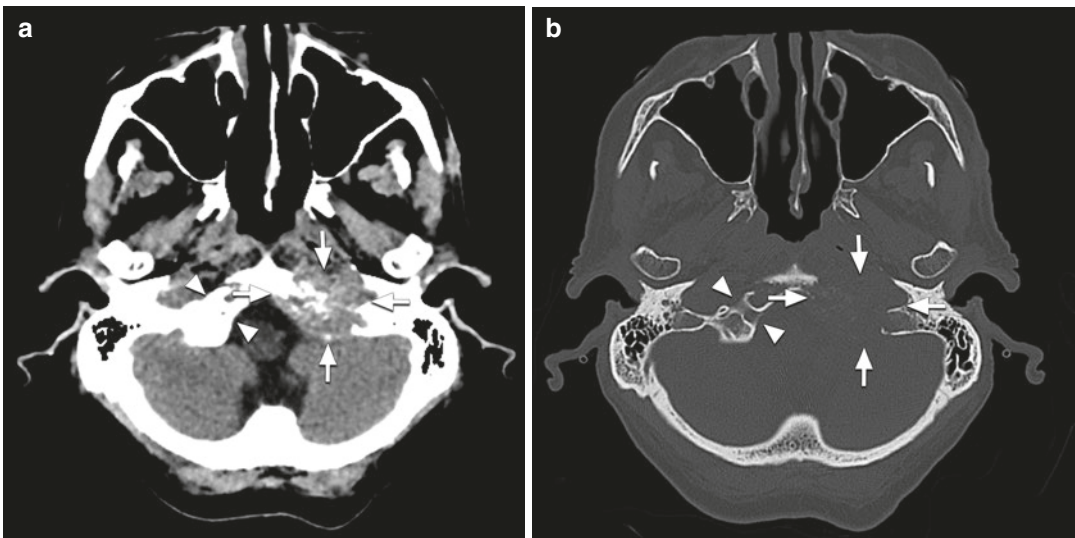


Fig. 2.20 Skull base destruction. Axial CT with (a) soft tissue window setting and (b) bone window setting. In a patient with known bronchial carcinoma, the skull base on

the left side is infiltrated by a lytic bone metastasis (arrows). On the contralateral side, the intact hypoglossal canal (arrowheads) can be seen

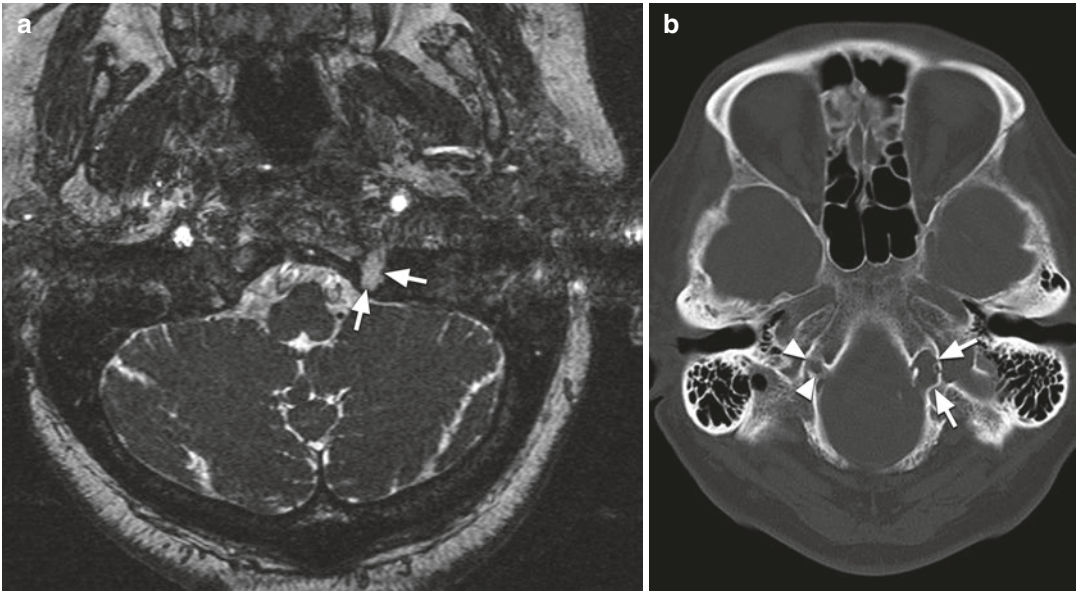


Fig. 2.21 Schwannoma. (a) Axial T2w MRI, (b) axial CT. Schwannoma of the hypoglossal nerve with scalloping of the hypoglossal canal (arrows). Regular hypoglossal canal on the asymptomatic side (arrowheads)

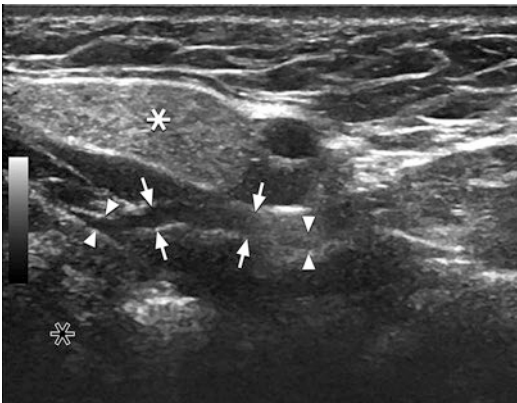


Fig. 2.22 Neurofibroma of the hypoglossal nerve. Longitudinal scan of the hypoglossal nerve at the mandibula. Marked thickening of the hypoglossal nerve due to a neurofibroma (arrows) in a patient with neurofibromatosis. Note the regular nerve caliber (arrowheads). Submandibular gland (white asterisk) and body of the tongue (black asterisk)

Cavernous Sinus/Cavernous Sinus Region/Parasellar Region

The region around the sella, and the parasellar region, contains a plethora of structures that are profoundly covered in the anatomy section of this book: the plexus of cavernous sinus veins; cranial nerves III, IV, V, and VI; sympathetic fibers; and the internal carotid artery.

As mapped out for each cranial nerve, selecting the best imaging modality depends on the clinical problem and the selected anatomical target.

In general, MRI with contrast—ideally in a high resolution—ensures a good overview.

For osseous, destructive processes, high-resolution CT with multiplanar reconstructions is recommended.

Regarding pathologies of the internal carotid artery, CT angiograms and MRI angiograms are the best modalities. In cases of suspected internal carotid artery fistulas, conventional angiography provides the insight of the vascular situation necessary for percutaneous interventional treatment.

Gasserian Ganglion/Semilunar Ganglion/Trigeminal Ganglion/Meckel's Cave

The trigeminal ganglion is located in the lateral wall of the above mentioned parasellar region. From here, the three branches of the trigeminal nerve leave in different directions. MRI with contrast is the best imaging modality to assess this region, granting a good overview.

MRI also plays a decisive role in detecting perineural spread of tumors from the masticatory space. CT may provide additional information on the aggressiveness of the tumor spread by assessment of potential bone destruction.

In the diagnostic workup of trigeminal neuralgia, MRI may confirm clinical suspicions, such as by depicting contrast enhancement in viral etiologies or deformation of the cisternal root by vascular loops [17] (Fig. 2.23).

Orbit

The orbit contains a multitude of different structures. By imaging of the orbit, a pathology should

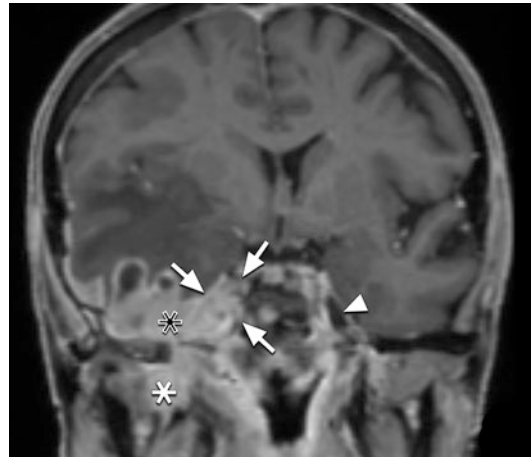


Fig. 2.23 Perineural tumor spread with infiltration of the trigeminal ganglion. Coronal T1w MRI with contrast. Squamous cell carcinoma tumor progression from below the skull base (white asterisk) into the neurocranium (black asterisk) infiltrating Meckel's cave (arrows). Here, the trigeminal ganglion is infiltrated and entirely contrast enhanced, while the ganglion can be seen as a hypointense structure (arrowhead)

first be assigned to a region, such as regarding the globe, the optic nerve, the myofascial cone, and the lacrimal gland.

MRI provides the best soft tissue contrast and allows a suppression of the fat tissue signal intensity (Fig. 2.24).

With ultrasound, it is easy to visualize the entire orbit, while CT depicts the osseous structures of the orbit, especially the bony orbital openings.

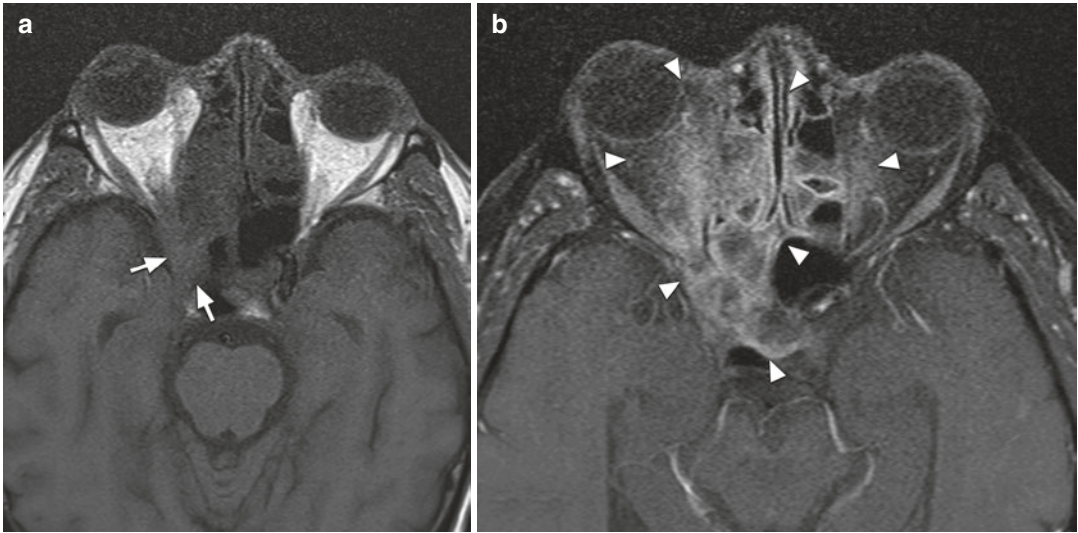


Fig. 2.24 Aspergilloma infiltration. (a) Axial T1w pre-contrast enhancement MRI, (b) Axial T1w MRI with contrast. Note the true extent of the aspergilloma infiltration

(arrowheads) after application of a contrast agent and the smaller visual impression before contrast (arrows)

References

- Meng S, Platzgummer H, Loizides A, Chang KV, Gruber H. Ultrasound of small nerves. *Ultraschall Med.* 2022;43(1):12–33.
- Abolmaali N, Gudziol V, Hummel T. Pathology of the olfactory nerve. *Neuroimaging Clin N Am.* 2008;18(2):233–42. preceding x
- Duprez TP, Rombaux P. Imaging the olfactory tract (cranial nerve #1). *Eur J Radiol.* 2010;74(2):288–98.
- Kendall CJ, Prager TC, Cheng H, Gombos D, Tang RA, Schiffman JS. Diagnostic ophthalmic ultrasound for radiologists. *Neuroimaging Clin N Am.* 2015;25(3):327–65.
- Becker M, Masterson K, Delavelle J, Viallon M, Vargas MI, Becker CD. Imaging of the optic nerve. *Eur J Radiol.* 2010;74(2):299–313.
- Liang C, Du Y, Lin X, Wu L, Wu D, Wang X. Anatomical features of the cisternal segment of the oculomotor nerve: neurovascular relationships and abnormal compression on magnetic resonance imaging. *J Neurosurg.* 2009;111(6):1193–200.
- Agarwal N, Ahmed AK, Wiggins RH 3rd, McCulley TJ, Kontzialis M, Macedo LL, et al. Segmental imaging of the trochlear nerve: anatomic and pathologic considerations. *J Neuroophthalmol.* 2021;41(1):e7–e15.
- Seeburg DP, Northcutt B, Aygun N, Blitz AM. The role of imaging for trigeminal neuralgia: a segmental approach to high-resolution MRI. *Neurosurg Clin N Am.* 2016;27(3):315–26.
- Haller S, Etienne L, Kovari E, Varoquaux AD, Urbach H, Becker M. Imaging of neurovascular compression syndromes: trigeminal neuralgia, hemifacial spasm, vestibular paroxysmia, and glossopharyngeal neuralgia. *AJNR Am J Neuroradiol.* 2016;37(8):1384–92.
- Price T, Fayad G. Abducens nerve palsy as the sole presenting symptom of petrous apicitis. *J Laryngol Otol.* 2002;116(9):726–9.
- Singh AK, Bathla G, Altmeyer W, Tiwari R, Valencia MP, Bazan C 3rd, et al. Imaging spectrum of facial nerve lesions. *Curr Probl Diagn Radiol.* 2015;44(1):60–75.
- Skolnik AD, Loevner LA, Sampathu DM, Newman JG, Lee JY, Bagley LJ, et al. Cranial nerve Schwannomas: diagnostic imaging approach. *Radiographics.* 2016;36(5):1463–77.
- Garcia Santos JM, Sanchez Jimenez S, Tovar Perez M, Moreno Cascales M, Lailhacar Marty J, Fernandez-Villacanas Marin MA. Tracking the glossopharyngeal nerve pathway through anatomical references in cross-sectional imaging techniques: a pictorial review. *Insights Imaging.* 2018;9(4):559–69.
- Sniezek JC, Netterville JL, Sabri AN. Vagal paragangliomas. *Otolaryngol Clin North Am.* 2001;34(5):925–39. vi
- Ong CK, Chong VF. The glossopharyngeal, vagus and spinal accessory nerves. *Eur J Radiol.* 2010;74(2):359–67.
- Meng S, Reissig LF, Tzou CH, Meng K, Grisold W, Weninger W. Ultrasound of the hypoglossal nerve in the neck: visualization and initial clinical experience with patients. *AJNR Am J Neuroradiol.* 2016;37(2):354–9.
- Malhotra A, Tu L, Kalra VB, Wu X, Mian A, Mangla R, et al. Neuroimaging of Meckel's cave in normal and disease conditions. *Insights Imaging.* 2018;9(4):499–510.